Catalysis Science & Technology

Accepted Manuscript

ROYAL SOCIETY OF CHEMISTRY

www.rsc.org/catalysis

Journal Name

ARTICLE

Aerobic Selective Oxidation of 5-Hydroxymethyl-furfural over Nitrogen-doped Graphene Material with 2,2,6,6-Tetramethylpiperidin-oxyl as Cocatalyst

Received 00th January 20xx,
Accepted 00th January 20xx

DOI: 10.1039/x0xx00000x

www.rsc.org/

Guangqiang Lv,[a,b] Hongliang Wang,[a] Yongxing Yang,[a] Xiao Li,[b, d] Tiansheng Deng,[a] Chengmeng Chen,[c] Yulei Zhu,[a,d] Xianglin Hou[a]*

Abstract

N-doped graphene materials with various types and quantities of N species were prepared via thermal treatment of graphene oxide in flowing NH_3, and their catalytic performances were tested in aerobic selective oxidation of 5-hydroxymethyl-furfural (HMF). A full HMF conversion and nearly 100% selectivity to DFF can be obtained under relatively mild reaction conditions (6 h, 100 °C, 1 atm air pressure) with 2,2,6,6-tetramethylpiperidin-oxyl (TEMPO) as co-catalyst. The reduction degree of graphene oxide in NH_3 was characterized by visible Raman spectroscopy. The amount and nature of doped nitrogen species were examined by X-ray photoelectron spectroscopy to reveal the genesis of active species by nitrogen doping. The graphitic nitrogen species doped into graphene lattice were demonstrated to be responsible for the activation of molecular oxygen. In selective oxidation of HMF, N-doped graphene showed much lower apparent activation energy (ca. 13.5 kJ mol^{-1}) compared with conventional active carbon supported metal catalysts (Ru/C, Pt/C, Pd/C, Au/C. 51-77 kJ mol^{-1}). Based on current results and previous reports, a possible reaction pathway with graphitic N species as active sites was proposed. This study examines the origin of the enhanced catalytic activity, which can be linked to the synergistic effect of TEMPO, N-doped graphene and molecular oxygen. This kind of synergistic effect makes the oxidation of HMF run smoothly. The present study demonstrates the potential of nitrogen-doped graphene material function as an efficient and alternative material to metal-based catalysts for organic synthetic reactions.

1. Introduction

Rapid depleting fossil fuels and escalating energy consumption coupled with rising environmental awareness among nations have led to increased focus on alternate, viable, eco-friendly and renewable energy sources.[1] This has stimulated research activities for the utilization of renewable and abundant biomass resources for the sustainable production of chemicals and liquid fuels.

5-Hydroxymethyl-furfural (HMF) is a promising platform compound derived from carbohydrates. It can be used as a versatile precursor for the production of fine chemicals, plastics, pharmaceuticals and liquid fuels.[2] Selective oxidation of HMF is one of the most pivotal transformations in the biorefinery.[3] The oxidation of HMF can generate several kinds of oxidation products such as 2,5-diformylfuran (DFF), 5-hydroxymethyl-2-furancarboxylic acid (HMFCA), 5-formyl-2-furancarboxylic acid (FFCA), and 2,5-furandicarboxylic acid (FDCA; Scheme 1).

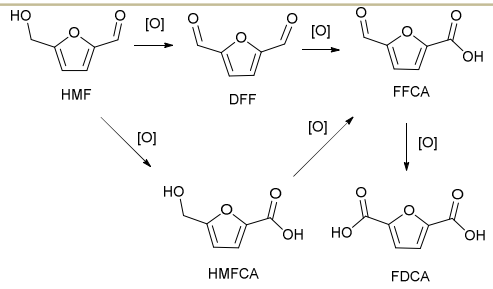

Scheme 1. Oxidation products of HMF

[a] Shanxi Engineering Research Center of Biorefinery, Institute of Coal Chemistry, Chinese Academy of Sciences, 27 South Taoyuan Road, Taiyuan 030001, People's Republic of China
[b] University of Chinese Academy of Sciences, Beijing, 100039 People's Republic of China.
[c] Key Laboratory of Carbon Materials, Institute of Coal Chemistry, Chinese Academy of Sciences, 27 South Taoyuan Road, Taiyuan 030001, People's Republic of China.
[d] State Key Laboratory of Coal Conversion, Institute of Coal Chemistry, Chinese Academy of Sciences,27 South Taoyuan Road, Taiyuan, People's Republic of China. 030001
† Fax: +86 351 4041153; Tel: +86 351 4049501, E-mail: houxianglin@sxicc.ac.cn (Xianglin Hou)
Electronic Supplementary Information (ESI) available: [details of any supplementary information available should be included here]. See DOI: 10.1039/x0xx00000x

FDCA is a highly promising bio-based building block for resins and polymers, thus can be usedas a promising replacement for terephthalic acid, a petroleum-based monomer in the plastics industry.[4-6] DFF, as another important oxidative product of HMF has received significant attention in recent years. It can be used for the synthesis of furan-containing polymers and materials with special properties and as starting materials for the synthesis of various poly-Schiff bases, pharmaceuticals, antifungal agents, organic conductors and cross-linking agents of poly (vinyl alcohol) for battery applications.[7] In the early reports, DFF has primarily been synthesized from the oxidation of HMF by using of stoichiometric oxidants, including NaOCl,[8] $BaMnO_4$,[9] and pyridinium chlorochromate.[10] These methods not only consumed stoichiometric oxidant but also produced large amounts of waste. In recent years, there is growing attention on the synthesis of DFF from the oxidation of HMF with molecular oxygen as terminal oxidant catalyzed by heterogeneous or homogeneous metal catalysts like Co/Ce/Ru,[1] Ru,[1, 11, 12] Cu/V,[13] Mn,[14] Mo/V,[15] V.[16, 17] Metal-containing catalysts usually give relatively high DFF yield. However, the transition –metal –based catalysts applied in oxidative transformation are difficult to remove, toxic and are frequently obtained from limited natural resources.[18]

Recently, metal-free materials have attracted increasing attention as sustainable alternatives to metal-based catalysts. In energy conversion and chemical synthesis, metal-free catalysts are expected to reduce the cost, prevent deactivation and facilitate mechanistic studies.[19] Extensive studies have been carried out on graphene-based hybrid materials in investigation of the potential applications of such materials in the fields of adsorption and catalysis. It is reported that the electronic structure of graphene can be significantly modified by the introduction of certain heteroatoms, such as N, B, P.[20, 21] Therefore, catalytic properties were altered as a consequence. Nitrogen-doped carbon nanotubes or graphene materials have been successfully applied in the aerobic oxidation of benzylic alcohols,[22] benzylic hydrocarbons, cyclooctane and styrene.[23] N-doped graphene has also been used in selective oxidation of cyclohexene,[24] non-radical catalytic oxidation of phenol,[19] epoxidation of trans-stilbene and styrene [25] and oxidation of ethylbenzene.[26] Hiroyuki Watanabe et.al [27] have reported that N-doped active carbon showed a mild catalytic activity in HMF oxidation (80 °C, 15 h, 72 wt.% loading of N-doped AC, 24 % HMF conversion, 93% DFF selectivity). In early report,[28] N-doped graphene also showed a weak catalytic activity in benzyl alcohol oxidation reaction.

TEMPO is a simple, organic oxidation catalyst capable of oxidizing a wide range of alcohols under mild conditions.[29-34] The mechanism of TEMPO proceeds through an initial electrochemical oxidation step from a stable nitroxyl radical to the catalytically active oxoammonium salt ; subsequent oxidation of the substrate results in a hydroxylamine, which is oxidized to the nitroxyl radical, completing the catalytic cycle.[32] To constitute an effective catalytic system in aerobic oxidation of HMF into DFF over nitrogen-doped graphene, homogeneous TEMPO was introduced to the reaction system as cocatalyst. In this work, a series of N-doped graphene materials with few layers and various types and quantities of nitrogen species are prepared by the high- temperature ammonia treatment method. It was observed that the selective oxidation of HMF with molecular oxygen as the terminal oxidant could be triggered over N-doped graphene. By XPS tests and other control experiments, we identified that the lattice nitrogen species that stayed at the graphitic site were responsible for the oxidation reaction.

2. Results and Discussion

2.1 Synthesis and Characterization of N-doped Graphene Nanosheet.

Thermal annealing of graphene oxide (GO) in ammonia reported by Dai et al.[35] is a facile route and, thus, used to obtain gram-scale NG materials in this work. In our preparation procedure, natural flake graphite as the starting material was first oxidized to graphite oxide by a modified Hummers methods. The details of synthesis are described in Supporting information. The obtained graphite oxide was thermal exfoliated in vacuum (25 torr) at ~200 °C for 4 hours. Four N-doped graphene samples (denoted as NG-T, where T means nitridation temperature) were prepared by a postnitridation of graphene oxide in flowing NH_3 atmosphere at a temperature ranging from 400 to 1000 °C. For comparison, two reduced but un-doped graphene samples were prepared by thermal treatment of GO in flowing He atmosphere at 400 °C and 800 °C for 4 h, respectively. All of the as-prepared samples were characterized by BET surface area analysis, transmission electron microscopy (TEM), scanning electron microscope (SEM), X-ray powder diffraction (XRD), X-ray Photoelectron Spectroscopy (XPS) and visible Raman spectroscopy. The exfoliated GO material has a BET surface area 340.6 m^2/g with an average pore diameter 14.3 nm. After nitridation, NG-T samples does not show much difference in the BET surface area and average pore diameter compared with starting GO sample (Table S1, Supporting Information).

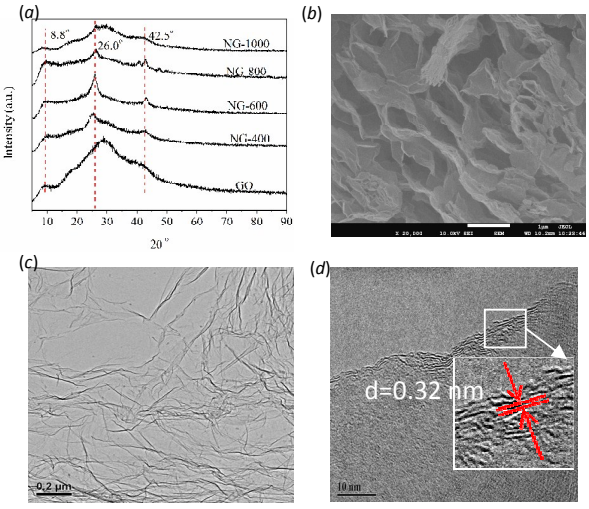

Fig. 1 Characterization of samples. (a) XRD patterns of the NG-T samples and garphene oxide; (b) SEM image of NG-800; (c) TEM image of NG-800. (d) HRTEM of NG-800

Fig. 1 *a* shows XRD patterns of the four NG-T samples and GO. Graphite oxide represents one main reflection peak centered at 11.3°, corresponding to the *c*-axis interlayer spacing of 0.81 nm (Fig. S1, Supporting Information). It indicates that graphite is oxidized completely. After exfoliated in vacuum at ~200 °C for 4 hours, the exfoliated GO shows one main broad peak at 28.8° (d=0.32 nm) and one weak peak centered at 8.8° (d=1.02 nm), suggesting that graphite oxide cannot be uniformly exfoliated under these conditions. All of NG-T samples show one main peak at 26.0° (0.32 nm) and two weak peaks at 8.8° (d=1.02 nm), 42.5° (d=0.21 nm). Compared with graphene oxide, the intensity of reflection peak at 26.0° decreased, as a result of the poorer crystallinity caused by the swelling of graphene sheets under high temperature and reduction atmosphere.

The morphology of GO and NG-T was determined by scanning electron microscope (SEM) and transmission electron microscopy (TEM) method (Fig. 1 b, c, d and Fig. S2, Supporting Information). SEM and TEM imaging of GO and NG-T all exhibit a randomly aggregated, crumpled nanostructure of graphene. After the introduction of nitrogen, the morphology of graphene sheets does not exhibit noticeable differences under SEM and TEM observation. HRTEM characterization further indicates that these nanosheets consist of 1-10 layer graphenes. The interlayer distance is about 0.32 nm, confirming the XRD results.

Thermal anneal of GO in ammonia is an efficient method for nitrogen dope and reduction of graphene oxide simultaneously. Oxygen groups in graphene oxide and anneal temperature are essential for reaction between graphene oxide and NH_3 for

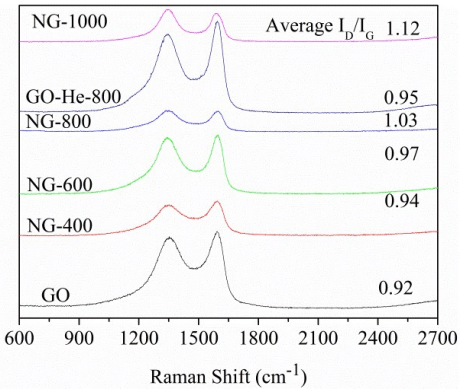

Fig. 2 Visible-Raman spectra of GO and NG-T samples

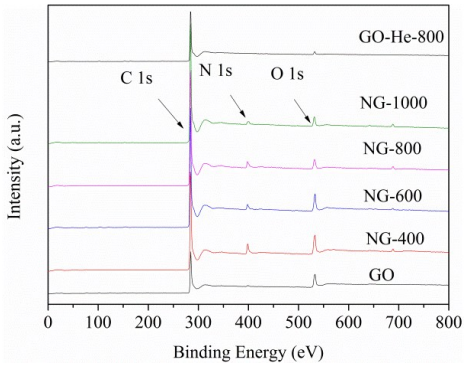

Fig .3 XPS patterns of GO and NG-T samples

substituted and covalent C-N bond formation.[35] Fig. 2 compares the Raman spectra of GO and NG-T samples. All samples display two intense bands. The D band (~1350 cm^{-1}), which as a breathing mode of *k*-point phonons of A_{1g} symmetry is attributed to local defects and disorders, particularly the defects located at the edges of graphene and graphite platelets. The G band (~1580 cm^{-1}) is generally assigned to the E_{2g} phonon of sp^2 bond of carbon atoms.[36] The larger I_D/I_G peak intensity ratio of a Raman spectrum indicates higher defects and disorders of the graphitized structures containing the disorders caused at the edges of the carbon platelets. Besides, intensity ratio of 2D band and D+G band located at ~2700-3000 cm^{-1} can also act as an indicator to judge the recovery of graphitic electronic conjugation.[37] In Fig. 2, the D band and G band display at about 1345 cm^{-1} and 1592 cm^{-1}, respectively. The I_D/I_G ratio increases from 0.92 for GO to 1.12 for NG-1000. The I_{2D}/I_{2G} ratio also increases from 0.91 for GO to 1.05 for NG-1000 (Fig S3, Table S2, Supporting Information). This increase can be assigned to the removal of oxygen functionalities and formation of the pores (as defects and disorders) in the graphene sheets. These results clearly show that thermal annealed GO in NH_3 under different temperatures are reduced efficiently to different level. Comparing the I_D/I_G ratio of NG-800 with GO-He-800, NH_3 shows more effective effects in GO reduction.

XPS is used to characterize the elemental composition of NG-T samples (Fig. 3). More than ~17 at % oxygen are remained after GO exfoliated and no nitrogen signal is observed in the GO XPS spectrum. Thermal annealed GO in flowing He at 800 °C shows a weak O 1s signal and no N 1s signal was observed. XPS spectra reveals that thermal anneal of GO in NH_3 induces a continued decrease of O content with the annealed temperature increasing. Element analysis indicates the C/O ratio of GO increases from 4.68 to 10.26, 13.31, 22.49, 24.28 respectively for NG-400, NG-600, NG-800 and NG-1000 (Table S2, Supporting Information). XPS reveals that N species are doped into graphene skeleton structure at all selected temperatures. After reaction with ammonia at a temperature range of 400-1000 °C, a new signal attributed to N 1s can be discerned from the XPS spectra, in addition to the O 1s and C 1s signal. It can be estimated roughly from the intensity of N 1s signal that the content of the N species decreases in the order NG-400 > NG-600 > NG-800 > NG-1000.

2.2 Catalytic Behavior of NG-T for Aerobic Oxidation of HMF.

In a preliminary experiment, 1 mmol HMF dissolved in 30 mL acetonitrile was heated to 100 °C for 3 h under 1 atm air condition in a 100 mL stainless autoclave. As shown in Table 1, NG-800 alone was a poor catalyst for the aerobic oxidation of HMF to DFF (entry 1) and slight amount of FFCA was detected. On the other hand, addition of TEMPO, which itself was not active as catalyst or oxidant (entry 2), to above NG-800 system led to a substantial increase in activity (entry 8).

To determine whether TEMPO combined NG-T materials can directly oxidize HMF to DFF, where TEMPO functioned as an oxidant, the aforementioned oxidation reaction was performed under an atmosphere of nitrogen. After 3 hours and 100 °C, a HMF conversion of 11.5% was achieved (entry 3). This result obvious demonstrated that oxygen was important and should be the terminal oxidant. The HMF conversion of 11.5% can be attributed

Journal Name

ARTICLE

Table 1. Oxidation of HMF into DFF over different catalyst [a]

Entry	Catalyst	Reaction time (h)	N (%)[b]	O (%)[b]	HMF Conv. (%)	DFF Selec.(%)
1[c]	NG-800	3	5.41	3.97	1.8	80.1
2[d]	---	12	---	---	2.1	71.4
3[e]	NG-800	3	5.41	3.97	11.5	80.0
4	GO	3	0	18.01	50.1	84.2
5[f]	GO-He-800	3	0	7.05	3.4	91.2
6	NG-400	3	6.51	7.83	76.6	98.8
7	NG-600	3	5.80	4.72	84.1	98.6
8	NG-800	3	5.41	3.97	89.9	98.5
9	NG-1000	3	3.10	2.92	80.7	98.7
10	NG-800	6	5.41	3.97	100	99.5

[a] Reaction conditions: HMF, 1 mmol, 126 mg; acetonitrile, 30 mL; TEMPO, 1 mmol, 155 mg; reaction time, 3 h; reaction temperature, 100 ^{o}C; catalyst, 100 mg; 1 atm air pressure in 100 mL stainless autoclave; stirring speed, 800 rpm.

[b] Determined by elemental analysis (wt.%).

[c] No TEMPO.

[d] No NG-T.

[e] N_2 atmosphere.

[f] Thermal reduced GO in flowing He atmosphere under 800 ^{o}C for 4 h was used.

to the contribution of dissolved oxygen in solvent and adsorbed oxygen, or can be attributed to the residual oxygen group function in NG-T materials.

When GO was used as the oxidation catalyst, a HMF conversion of 50.1% with 84.2 % selectivity to DFF were observed (Table 1, entry 4).This results have been discussed in our other work, carboxylic acid groups in GO were demonstrated to be direct oxidants first. After the GO was partially reduced in reaction processing, the partially reduced GO (rGO), as a carbocatalyst, showed catalytic activity in HMF aerobic oxidation.[38] With GO as a carbocatalyst, a high HMF conversion also can be reached. However, the reaction time needed was long (12 h, 89.4 % HMF conversion with 98.8% selectivity to DFF). Elemental analysis shows that the O content in GO-He-800 decreased to ca. 7.05 wt % and O content in NG-400, NG-600, NG-800, and NG-1000 decreased to 7.83, 4.72, 3.97, 2.92 wt %, respectively. When GO-He-800 was employed in the reaction, a relatively low HMF conversion was observed in 3 h (Table 1, entry 5), this result indicates that residual oxygen groups in GO-He-800 have almost lost its catalytic or oxidant activity here. The obvious lower quantity of oxygen content in NG-800 than that in GO-He-800 indicates NH_3 is more effective than He in GO reduction. According to this result, we suggest that the enhanced catalytic activity of NG-T origin from the doped N, rather than the residual oxygen groups in NG-T materials. After GO was treated in ammonia at 400 ^{o}C (NG-400), 6.51 wt % nitrogen species were incorporated into the skeleton structure of graphene. The HMF conversion increased to 76.6% (Table 1, entry 6). This demonstrates that ammonia treatment of GO is beneficial to its catalytic reactivity.

From XPS results in Fig. 3 and elemental analysis in Table 1, it can be found that the N contents in NG-T decreased with the treatment temperature increasing. However, the catalytic activity increased with treatment temperature increasing (Table 1, entry 6, 7, 8). When NG-600 and NG-800 were employed in the reactions, an continuous improvement in their catalytic performance were observed, that is, the HMF conversion increased to 84.4% (NG-600, Table 1, entry 7) and 89.9% (NG-800, Table 1, entry 8) with no decrease in DFF selectivity. When the reaction time was prolonged to 6 h, a full HMF conversion with 99.5% DFF selectivity over NG-800 was achieved (Table 1, entry 10). After GO was thermal annealed with ammonia at 1000 ^{o}C, elemental analysis reveals that only 2.92 wt % N were remained in NG-1000. The HMF conversion showed a slight decrease compared to that with NG-800 as catalyst (Table 1, entry 9). Above results demonstrate that by thermal treatment in NH_3, the catalytic performance of N-doped graphene catalyst can be adjusted by varying the thermal treatment temperature. With nitrogen doping temperature increased in NG preparation, (400, 600, 800 and 1000 ^{o}C), continuously drops in the total nitrogen content in NG-T materials were observed (Table 1). We need to note that at the same time over NG-T materials, instead, the catalytic performance increased first and then decreased again, NG-800 showed the best catalytic performance.

2.3 Chemical States of N Species Doped in Multilayer Graphene.

To understand the catalytic phenomenon, chemical states of these N species doped into the flat lattice of graphene were characterized in detail by XPS. The atomic content of C, N and O elements in these samples calculated from XPS spectra (Fig. 3) is summarized in Table

2. The bonding configurations of N species in these N-doped multilayer graphenes were further studied on the basis of high-resolution XPS spectra. Their molecular bonding structures were depicted in Fig. 4 a. As shown in Fig. 4 b, the N 1s peaks in the high-resolution XPS can be fitted into three peaks corresponding to three types of N species in these NG-T nanosheets. According to previous studies,[28, 39-41] the binding energy of 398.1 eV was ascribed to pyridinic N (N_1), and the binding energy of 399.4 eV was attributed to pyrrolic N (N_2), the peak at 401.7 eV corresponded to graphitic N (N_3). It can be seen from Fig. 3 and Table 2 that the N atomic total content decreased monotonically from 6.07 to 2.42 at % with the treatment temperature increased from 400 to 1000 ^{o}C. It also should be note that pyridinic and pyrrolic N species (N_1+N_2) were predominant in these NG-T samples. N_1 or N_2 species showed a monotonically decrease with treatment temperature increasing, similar to the total nitrogen content. However, graphitic N species contents showed an increase from 0.14 to 1.22 at % while the treatment temperature increasing from 400 to 800 ^{o}C, and decreased from 1.22 to 0.92 at % when temperature increased to 1000 ^{o}C, indicating that there was an optimal temperature for the formation of N_3 species.[35] This phenomenon was consistent with the catalytic activity changing of NG-T samples in HMF oxidation reaction. In nitridation, oxygen functional groups in GO were responsible for reactions with NH_3 to form C-N bonds and afforded N-doped NG-T materials. Under relatively low temperature (≤500 ^{o}C), carboxyl, lactone and carbonyl groups can be reduced, reaction of oxygen groups with NH_3 resulting in formation of pyridinic N and pyrrolic N. Phenol and quinone groups were decomposed almost entirely between ~500 - 900 ^{o}C.[35] Above ~900 ^{o}C, hydroxyl and epoxy groups in GO basal plane reacted with NH_3 leading to the formation of graphitic N, i.e. N that replaced the carbon atom in the graphene sheets and bonded to three carbon atoms. At relatively high treatment temperature, the distribution of nitrogen in graphene was governed by the balance between nitrogen removal/dope due to the high temperature treatment and/or reconstruction of nitrogen among different sites.[25] This resulted in the decrease of total N content among NG-T samples with increasing the treatment temperature. Fig. 4 c displays the high-resolution O 1s XPS spectra of the NG-T and GO-He-T samples. The broad O 1s peak can be divided into three peaks centered at ~530.6, 532.2 and 533.3 eV. According to the literatures,[41, 42] the two peaks centered at ~530.6 and 533.3 eV belong to C=O and C-OH or C-O-C, respectively. Data in Table 2 shows that O content in hydroxyl or epoxy groups types (O_3) in NG-T decrease in an level that less than that of carbonyl and carboxyl groups (O_1, O_2) when the treatment temperature below 600 ^{o}C. This result is consistent with above analysis that the N doped into graphene below 600 ^{o}C stayed in pyridinic and pyrrolic type mostly. However, the assignment of the binding energy of ~532.2 eV seems to be not straightforward. It may be contributed from both adsorbed oxygen or carboxyl groups in GO.[28] But for NG-T which were treated in high temperature NH_3, it is believed that the peak at ~532.2 eV belongs only to the adsorbed oxygen, because the acid-base reaction of –COOH +NH_3 = O=C-NH_2 +H_2O can consume the residual –COOH completely.[28] For comparison, high-resolution O 1s XPS spectra of thermal reduced GO in flowing He atmosphere at 400 ^{o}C and 800 ^{o}C were shown in Fig. 4 d. XPS of GO-He-T and datas in Table 2 show that GO-He-400 remained relatively high amount of carboxyl oxygen groups (5.67 at %). Increasing the reduction temperature to 800 ^{o}C, the carboxyl

Table 2. Distribution of element species obtained from the de-convolution of the N 1s, O 1s peaks by XPS

Entry	Binding Energy(eV)	at %						
		GO	GO-He-400	GO-He-800	NG-400	NG-600	NG-800	NG-1000
Total carbon (C)		82.12	87.21	94.31	85.58	90.46	91.76	93.73
Total nitrogen (N)					6.07	4.39	4.16	2.42
Pyridinic nitrogen (N_1)	~398.1				3.09	2.20	1.77	0.77
Pyrrolic nitrogen (N_2)	~399.4				2.10	1.23	1.17	0.73
Graphitic nitrogen (N_3)	~401.7				0.14	0.95	1.22	0.92
Total oxygen (O)		17.88	12.79	6.69	8.34	5.15	4.08	3.86
Oxygen of C=O (O_1)	~530.6	4.80	3.50	2.08	2.47	1.40	1.44	1.61
Adsorbed oxygen (O_2)	~532.2	7.81 [a]	5.67 [a]	3.46 [a]	2.24	2.26	1.33	1.35
Oxygen of C-O or C-O-C (O_3)	~533.3	5.37	3.62	1.15	3.64	3.09	1.31	0.9
N/C (at. %)					7.09	4.94	4.53	2.58
N_1/C (at. %)					3.61	2.47	1.93	0.82
N_2/C (at. %)					2.45	1.38	1.28	0.77
N_3/C (at. %)					0.16	1.07	1.33	0.98
O/C (at. %)		21.77			9.75	7.6	4.44	4.12
O_1/C (at. %)		5.85			2.89	1.58	1.57	1.72
O_2/C (at. %)		9.51			2.62	2.54	1.45	1.44
O_3/C (at. %)		6.54			4.25	3.48	1.43	0.96

[a] Oxygen of HO-C=O.

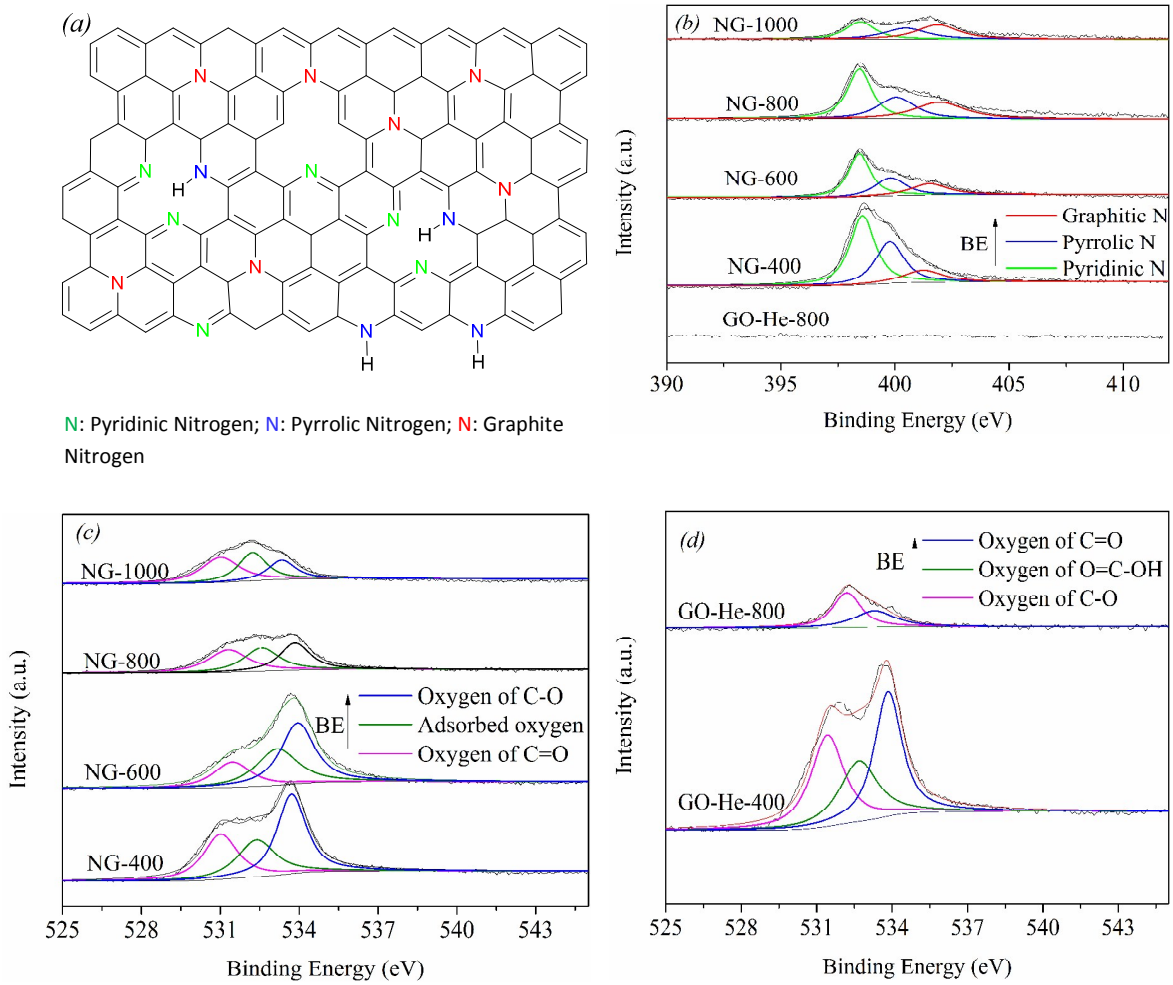

Fig. 4 (a) Chemical states of N species in NG-T samples. (b) High-resolution N 1s XPS spectra of the NG-T samples (c) High-resolution O 1s XPS spectra of the NG-T samples and (d) High-resolution O 1s XPS spectra of the samples.

oxygen content decreased to a relatively low level (3.46 at %), however, it still remained high than that in NG-400 (2.24 at %). The obvious lower quantity of O content in carboxyl type (or should be attributed to adsorbed oxygen here) in NG-400, compared with GO-He-400 and GO-He-800, demonstrated the acid-base reaction effect (Table 2).

However, on the basis of elemental analysis and ICP results, we notice that, in addition of carbon, nitrogen and residual oxygen, the NG-T samples contain an impurity of manganese. As shown in Table S3, NG-T materials contained around 310-350 ppm Mn. It has been demonstrated that manganese in active state (Mn_3O_4) has the catalytic ability in aerobic oxidation of HMF.[14] Mn-based impurities were also demonstrated to be a key factor that showed important influence on the oxygen reduction reaction.[43] However, because manganese and nitrogen coexist on NG-T samples, it is unclear whether it is manganese or nitrogen alone or their combination that generate the catalytic activity.

To check whether manganese component was crucial for the reactivity in the HMF oxidation reaction, the NG-1000 sample was washed with HCl solution completely,[44] decreasing the Mn content to ~37 ppm. On another side, 0.34, 0.68 and 1.02 wt % Mn/NG-1000 were prepared by impregnation method, where the contents were around 10, 20 and 30 times of that in NG-1000 ($KMnO_4$ as Mn resource and following thermal treatment at 1000 °C in flowing NH_3 were used to make the chemical state similar to residual Mn component in NG-T). The catalytic results are shown in Table S3, catalytic tests of the washed NG-1000 or supported Mn with NG-1000 as support showed no obvious change in HMF conversions. These results implied that the catalytic activity of NG-T was not affected by the Mn content. The Mn element in NG-T was not the catalytic center and did not work synergistically with N dopant in NG-T to produce the catalytic activity.

Compared with graphene, the heteroatom-doped graphene materials (including O, N, P, B et al.) often own a changed electron structure. The intrinsic change in electron structure of graphene induced by incorporation of heteroatoms will bring about some unique chemical properties, like catalytic effect. The reduction of GO restores its π-network and converts it to a semimetal.[21] Defect-less graphene has been frequently found to be inactive to promote aerobic oxidation.[45] Defects and nanovoids created in the basal

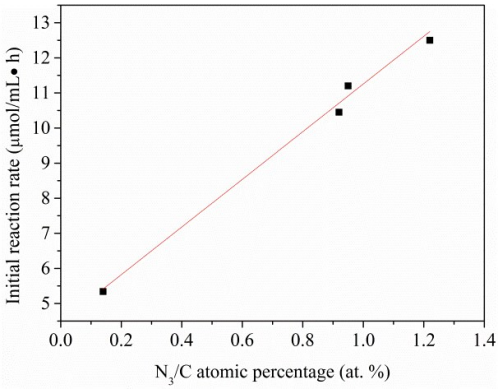

Fig. 5 Relationship between initial reaction rate and N_3 species in N-doped graphene.

plane of GO due to the loss of carbon atoms during thermal reduction are advantageous in catalysis because molecular species can be trapped and activated at these defects.[21] Considering the catalytic activity of various NG materials in Table 1, that is, the decreased order of catalytic activity: NG-800 > NG-600 > NG-1000 > NG-400 and NG-800 >>GO-He-800, it can be concluded that the aerobic HMF oxidation taking place on the NG-T samples originated predominantly from the catalysis of N dopant. The N dopant should be the catalytic active component, instead of C elements, whereas, the catalytic contribution from NG-T defects, including reactive edges, corners and carbene cannot be excluded completely for the transformation of HMF into DFF.[21, 45]

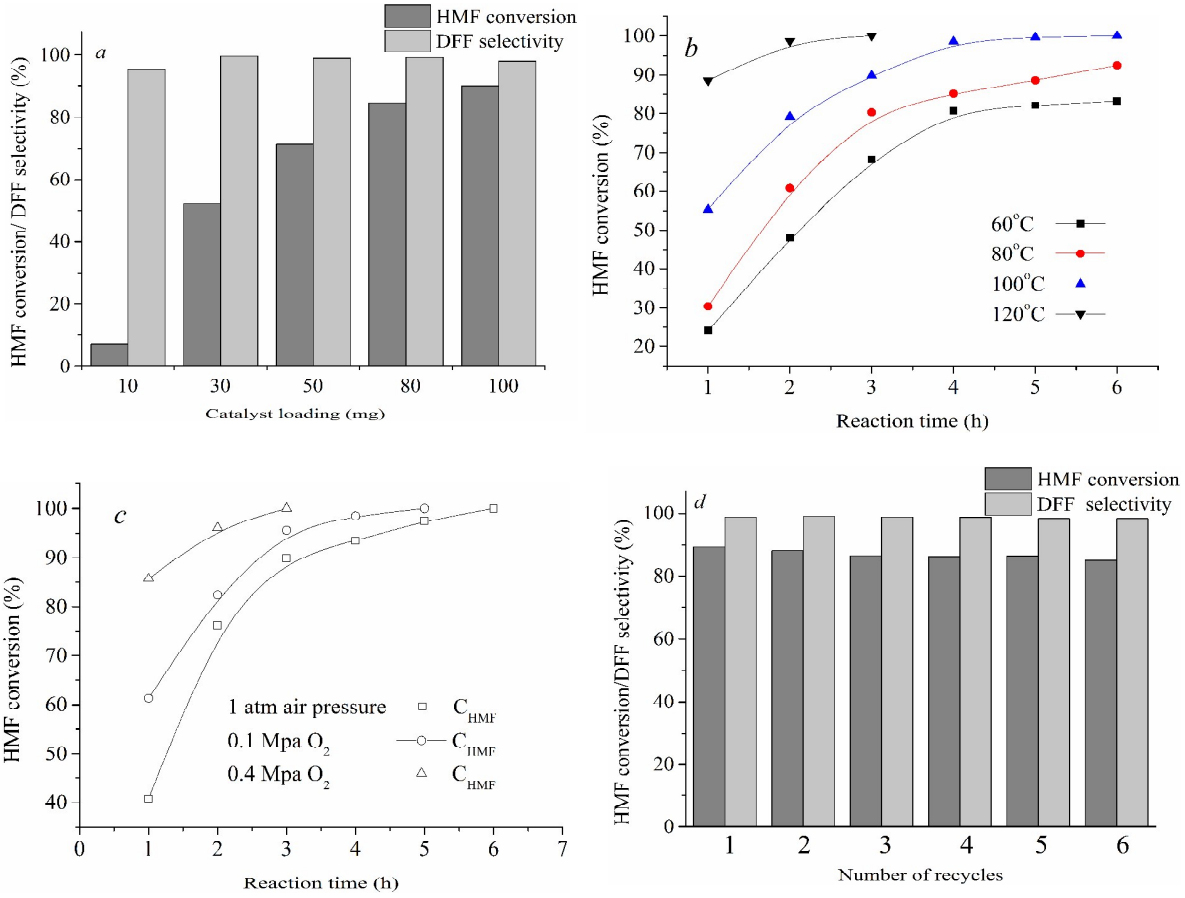

Fig. 6 Catalytic behaviour of NG-800 on aerobic oxidation of HMF into DFF under different conditions. (*a*) Effect of NG-800 loading on HMF conversion. HMF, 1 mmol, 126 mg; acetonitrile, 30 mL; TEMPO, 1 mmol, 155 mg; reaction time, 3 h; reaction temperature, 100 °C; 1 atm air pressure in 100 ml autoclave; stirring speed, 800 rpm. (*b*) Effect of the reaction temperature on HMF conversion. HMF, 1 mmol, 126 mg; acetonitrile, 30 mL; TEMPO, 1 mmol, 155 mg; NG-800, 100 mg; 1 atm air pressure in 100 mL autoclave; stirring speed, 800 rpm.(*c*) Effect of oxygen pressure on HMF conversion. HMF, 1 mmol, 126 mg; acetonitrile, 30 mL; TEMPO, 1 mmol, 155 mg; NG-800, 100 mg; stirring speed, 800 rpm. (*d*) Recycle ability of NG-800. HMF, 1 mmol, 126 mg; acetonitrile, 30 mL; TEMPO, 1 mmol, 155 mg (fresh TEMPO with used NG-800 catalyst were added into reaction mixture for every run); reaction time, 3 h; reaction temperature, 100 °C; 1 atm air pressure in 100 mL autoclave; NG-800, 100 mg; stirring speed, 800 rpm.

Journal Name

ARTICLE

The incorporated graphitic N concentrations in NG-T materials show a similar trend along with the varying of NG-T catalytic activity. The NG-600 and NG-800 that have the relatively high population of graphitic N possess the best catalytic performance in aerobic oxidation of HMF. Indeed, when we tried to correlate the catalytic activity with the concentration of N species in NG-T samples, we observed a linear relationship between the graphitic nitrogen concentration and the activity (Fig. 5). But, for the other two kinds of N species, pyridinic N (N_1) and pyrrolic N (N_2), no such correlation can be established (Fig. S4, Supporting Information). These results demonstrate that the graphitic N was responsible for the high catalytic activity in aerobic oxidation of HMF over NG-T materials. It is reported that the doped graphitic nitrogen have the function that modulate the electronic structure of sp^2 carbon material. The density of states intensities near the Fermi level for the adjacent ortho-carbon are much stronger than those of un-doped graphene carbon, which confers the nitrogen-neighboring carbon a metal-liked band electronic structure and makes the adjacent carbon more capable to host the formation of reaction oxygen species.[25]

2.4 Aerobic Oxidation of HMF into DFF under Different Conditions

The catalytic aerobic oxidation of HMF into DFF over NG-800 with TEMPO as co-catalyst under different conditions was investigated. Control experiments show that catalytic system without TEMPO gave a low HMF conversion (Table 1, entry 1). The effect of the TEMPO concentration on the rate of HMF oxidation was investigated (Fig. S5, Supporting Information). An almost linear increase of the total HMF conversion was observed with TEMPO concentration increasing in the reaction. Above 0.7 mmol quantity of TEMPO was used in the reaction system, the rate increase started to level out, and further addition of TEMPO led to only a minor increase in the HMF conversion after 1 h. To exclude the impact of TEMPO on the HMF transformation, an excess amount of 1 M mol quantity of TEMPO was used in following NG-800 catalytic ability tests. In Fig. 6 a-c, the results show that, as expected, the total HMF conversion increased with the amount of catalyst, reaction temperature and oxygen pressure increasing under all investigated time. Importantly, the DFF selectivity remained at relatively constant and high level (>95%) while the conditions varied (not shown in Fig. 6 *b*, *c*). This result suggests that NG-TEMPO catalytic system have a unique advantage in catalytic oxidation of HMF into DFF**.** Fig. 6 *d* illustrates the recycle ability of NG-800 in catalytic aerobic oxidation of HMF. To evaluate the recycle ability of NG-800 material in reaction, fresh and excess amount of TEMPO (1 M mol) with used NG-800 catalyst were added into the reaction mixture in every cycle. The HMF conversion and DFF selectivity showed only slight decrease and HMF conversion remains above 80% during reusing of NG-800 in six times. XPS characterization of recycled NG-800 for six times showed no obvious change in N-doping level. The morphology of used NG-800 after 6 cycles showed no noticeable differences under SEM and TEM observation (Fig. S6, Supporting Information). It is speculated that the slight loss of catalytic activity resulted from the deactivation of graphitic nitrogen species in NG-800 by gaseous oxygen or produced water during reaction, as indicated in literature.[27] There is also a problem should be noted that high loading of NG-T is employed to ensure a good HMF conversion (up to 80 wt %), which is also noted in other catalytic reactions with functionalized graphene as carbocatalyst.[21, 46]

2.5 Effect of Solvent on HMF Oxidation

The effect of solvent on the aerobic oxidation of HMF into DFF was investigated and summarized in Table 3. Table 3 shows that HMF conversion and DFF selectivity were affected greatly by the solvents. Generally, the effects of these solvent on HMF oxidation were complicated because of their dependence on the catalyst properties and reaction conditions.[4] In addition, the properties of the solvents, such as polarity, dielectric property, steric hindrance, and acid-base properties, also have great effect on the oxidation reaction.[4] In polar solvents, different HMF transformation behaviors were observed (Table 3, entry 1-6). Water –which from a sustainability viewpoint would be preferred-also showed a relatively high HMF conversion but a lower DFF selectivity (Table 3. entry 2). In polar protic solvents, water, methanol gave a much lower DFF selectivity than other solvents and large amount of FFCA was observed (Table 3, entry 2, 3). High HMF conversion and DFF selectivity were observed over NG-800 in other selected solvents (Table 3, entry 4-8) with slight amount of FFCA was produced. This implied that NG-800 was effective in various solvents in aerobic oxidation of HMF into DFF. Importantly, as DMSO and MIBK were often used as solvent in the production of HMF from fructose, graphene materials with strong acid and redox catalyst properties

Table 3. Results of the aerobic oxidation of HMF in various solvents over different catalysts [a]

Entry	Solvent	C_{HMF}(%)	S_{DFF}(%)	S_{FFCA}(%)
1	Acetonitrile	89.6	99.7	0
2	Water	85.7	46.4	45.8
3	Methanol	88.4	40.4	56.1
4	DMSO	100	94.4	4.3
5	DMF	95.6	92.8	2.3
6	MIBK	85.6	97.1	0
7	Toluene	99.5	95.2	0
8	Dichloromethane	88.5	84.5	5.5

[a] Reaction condition: HMF, 1 mmol, 126 mg; NG-800, 100 mg; TEMPO, 1 mmol, 155 mg; solvent, 30 mL; reaction temperature, 100 ^{o}C; 1 atm air pressure in 100 mL autoclave; stirring speed, 800 rpm; reaction time, 3 h.

show the potential as the metal-free catalyst for the synthesis of DFF from fructose by two consequence steps, which compromise the production of HMF from fructose and the subsequent oxidation of HMF.

2.6 Kinetic Analysis of Aerobic Oxidation of HMF into DFF over NG-800.

To illustrate the catalytic activity of this catalytic system, kinetic analysis was studied. The apparent activation energy was determined to be 13.5±0.8 kJ ● mol^{-1}, smaller much than that with Ru/C as catalyst, in which E_a was estimated to be 51±1 kJ ● mol^{-1}.[12] For the Ru/C catalyst, the TOF was 61.2 h^{-1} with the DFF selectivity up to 96.2% was reached. For the nitrogen-doped graphene, the graphitic N species can be assumed to contribute to the formation of active sites, so the TOF can be determined roughly using the number of these species determined by XPS. The TOF value obtained in this method was ca. 142.1 h^{-1} for NG-800 with a >98% DFF selectivity was achieved. The TOF for N-doped graphene was much higher than that of Ru/C. In GO/TEMPO catalytic system,[38] based on the determined active cites, that is, the carboxylic acid groups in GO material, the TOF was estimated to be ca. 3.09 h^{-1}. The nitridation of graphene oxide make the doped graphitic nitrogen species the new active sites in functioned graphene material and the TOF values enhanced significantly. These results suggest that the N-doped graphene can be an effective carbon-based catalyst in aerobic oxidation of HMF, the performance of NG/TEMPO system is comparable or even superior to that of metal catalysts.

2.7 Possible Reaction Pathways for Aerobic Oxidation of HMF.

Considering the reaction conditions in aerobic oxidation of HMF and previous work on N-doped active carbon and N-doped graphene,[27, 28] a possible reaction pathway was proposed as follows (Fig. 7): An oxygen molecule dissolved in the medium was adsorbed on a carbon site adjacent to the graphitic type nitrogen and/or on the the nitrogen atom. Then molecular oxygen was activated and the TEMPO was oxidized into oxoammonium cation (1), HMF was oxidized by oxoammonium cation with DFF produced, and the produced hydroxylamine (2) was re-oxidized by activated oxygen to regenerate molecular TEMPO. Sequentially, TEMPO was oxidized to oxoammonium cation (1) by activated molecular oxygen over active sites in NG-800 and participated into the next catalytic cycle.

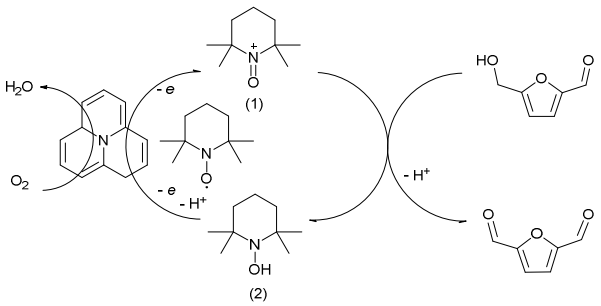

Fig. 7 Possible Reaction Pathway for Aerobic Oxidation of HMF in NG-TEMPO catalytic system with molecular oxygen as the terminal oxidant.

3. Conclusion

Above all, in the aerobic oxidation of HMF into DFF over GO catalyst, the carboxylic acid groups at the edges of defects, along with the localized unpaired electrons, worked synergistically to afford enhanced kinetics for the trapping and activation of molecular oxygen and TEMPO by a sequence of electron transport from TEMPO to molecular oxygen.[38] After the GO was thermal treated in flowing NH_3, the oxygen groups connected to graphene nanosheet by dangling bond were removed mostly, and the N species were doped into the graphene lattice structure by covalent C-N bonds and restored its π-network and converted it to a semimetal. The doped graphitic nitrogen species have the function of modulating the electronic structure of sp^2 carbon material. The enhanced density of states intensities near the Fermi level for the adjacent ortho-carbon in NG confers the nitrogen-neighboring carbon a metal-liked band electronic structure and thus makes the adjacent carbon more capable to host the formation of reaction oxygen species.

The nitrogen-doped, metal-free graphene is active for the aerobic selective oxidation of HMF to the DFF, with the TEMPO as the co-catalyst. By nitrogen-doping, different types of nitrogen species-pyridinic N, pyrrolic N and graphitic N are formed during thermal annealing in flowing NH_3. The amount and type of doped N species into NG-T materials can be controlled by controlling the annealing temperature. The graphitic N species are involved in the genesis of catalytically active sites, which should be a crucial effect in adsorbing and activating the oxygen molecules. This is the first report for the N-doped graphehe employing into the efficient selective oxidation of HMF into DFF. With graphene material prepared from various saving precursors, such as hydrocarbons, graphite and biomass, applying of carbon-based catalyst is believed to be a very promising alternative to the metal-based catalyst in fine chemical synthesis reactions.

Acknowledgements

This work was financially supported by the National Natural Science Foundation of China (NNSFC) (Grant 21403273), the National Key Basic Research Program of China (No.2012CB215305) and Science Foundation of Shanxi Province (2013011010-6).

References

1. Y. Wang, B. Liu, K. Huang and Z. Zhang, *Ind. Eng. Chem. Res.,* 2014, 53, 1313-1319.
2. A. A. Rosatella, S. P. Simeonov, R. F. M. Frade and C. A. M. Afonso, *Green Chem.,* 2011, 13, 754-793.
3. C. Moreau, M. Naceur Belgacem, N. Belgacem and A. Gandini, *Top. Catal.*, 2004, 27, 11-30.
4. Z. Zhang, Z. Yuan, D. Tang, Y. Ren, K. Lv and B. Liu, *ChemSusChem,* 2014, 7, 3496-3504.
5. X. Wan, C. Zhou, J. Chen, W. Deng, Q. Zhang, Y. Yang and Y. Wang, *ACS Catal.,* 2014, 4, 2175-2185.

6. B. Saha, D. Gupta, M. M. Abu-Omar, A. Modak and A. Bhaumik, *J.Catal.,* 2013, 299, 316-320.
7. -
8. A. S. Amarasekara, D. Green and E. McMillan, *Catal. Commun.,* 2008, 9, 286-288.
9. F. W. Lichtenthaler, *Acc. Chem. Res.,* 2002, 35, 728-737.
10. S. Tetsuro, U. Shinichi, S. Takaaki and S. Kenichi, *J. Heterocyclic Chem.,* 1995, 32, 727-730.
11. C. A. Antonyraj, J. Jeong, B. Kim, S. Shin, S. Kim, K.-Y. Lee and J. K. Cho, *J. Ind. Eng. Chem.,* 2013, 19, 1056-1059.
12. J. Nie, J. Xie and H. Liu, *J. Catal.,* 2013, 301, 83-91.
13. N.-T. Le, P. Lakshmanan, K. Cho, Y. Han and H. Kim, *Appl. Catal., A,* 2013, 464-465, 305-312.
14. B. Liu, Z. Zhang, K. Lv, K. Deng and H. Duan, *Appl. Catal., A,* 2014, 472, 64-71.
15. R. Liu, J. Chen, L. Chen, Y. Guo and J. Zhong, *ChemPlusChem,* 2014, 79, 1448-1454.
16. C. A. Antonyraj, B. Kim, Y. Kim, S. Shin, K.-Y. Lee, I. Kim and J. K. Cho, *Catal. Commun.,* 2014, 57, 64-68.
17. I. Sádaba, Y. Y. Gorbanev, S. Kegnaes, S. S. R. Putluru, R. W. Berg and A. Riisager, *ChemCatChem,* 2013, 5, 284-293.
18. D. R. Dreyer, H. P. Jia, A. D. Todd, J. Geng and C. W. Bielawski, *Org. Biomol. Chem.,* 2011, 9, 7292-7295.
19. X. Duan, H. Sun, Y. Wang, J. Kang and S. Wang, *ACS Catal.,* 2014, 553-559.
20. X. Wang, X. Li, L. Zhang, Y. Yoon, P. K. Weber, H. Wang, J. Guo and H. Dai, *Science,* 2009, 324, 768-771.
21. C. Su and K. P. Lou, *Acc. Chem. Res.,* 2013, 46, 2275-2285.
22. J. Luo, F. Peng, H. Wang and H. Yu, *Catal. Commun.,* 2013, 39, 44-49.
23. A. Dhakshinamoorthy, A. Primo, P. Concepcion, M. Alvaro and H. Garcia, *Chem.-Eur. J.,* 2013, 19, 7547-7554.
24. Y. Cao, H. Yu, F. Peng and H. Wang, *ACS Catal.,* 2014, 4, 1617-1625.
25. W. Li, Y. Gao, W. Chen, P. Tang, W. Li, Z. Shi, D. Su, J. Wang and D. Ma, *ACS Catal.,* 2014, 4, 1261-1266.
26. C. Ricca, F. Labat, N. Russo, C. Adamo and E. Sicilia, *J. Phys. Chem. C.,* 2014, 118, 12275-12284.
27. H. Watanabe, S. Asano, S.-i. Fujita, H. Yoshida and M. Arai, *ACS Catal.,* 2015, 5, 2886-2894.
28. J. Long, X. Xie, J. Xu, Q. Gu, L. Chen and X. Wang, *ACS Catal.,* 2012, 2, 622-631.
29. C. Bolm, A. S. Magnus and J. P. Hildebrand, *Org. Lett.,* 2000, 2, 1173-1175.
30. M. Zhang, C. Chen, W. Ma and J. Zhao, *Angew. Chem. In.t Ed.,* 2008, 47, 9730-9733.
31. B. Karimi, H. M. Mirzaei and E. Farhangi, *ChemCatChem,* 2014, 6, 758-762.
32. D. P. Hickey, R. D. Milton, D. Chen, M. S. Sigman and S. D. Minteer, *ACS Catal.,* 2015, 5, 5519-5524.
33. A. Dijksman, A. Marino-González, A. Mairata i Payeras, I. W. C. E. Arends and R. A. Sheldon, *J. Am. Chem. Soc.,* 2001, 123, 6826-6833.
34. I. A. Ansari and R. Gree, *Org. Lett.,* 2002, 4, 1507-1509.
35. G. Lv, H. Wang, Y. Yang, T. Deng, C. Chen, Y. Zhu and X. Hou, *ACS Catal.,* 2015, 5, 5636-5646.
36. X. Li, H. Wang, J. T. Robinson, H. Sanchez, G. Diankov and H. Dai, *J. Am. Chem. Soc.,* 2009, 131, 15939-15944.
37. A. Omid, *ACS Nano,* 2010, 4, 4174-4180.
38. D. Zhan, Z. Ni, W. Chen, L. Sun, Z. Luo, L. Lai, T. Yu, A. T. S. Wee and Z. Shen, *Carbon,* 2011, 49, 1362-1366.
39. H. Sun, Y. Wang, S. Liu, L. Ge, L. Wang, Z. Zhu and S. Wang, *Chem. Commun. (Camb),* 2013, 49, 9914-9916.
40. B. Guo, Q. Liu, E. Chen, H. Zhu, L. Fang and J. R. Gong, *Nano Lett.,* 2010, 10, 4975-4980.
41. D. Yang, A. Velamakanni, G. Bozoklu, S. Park, M. Stoller, R. D. Piner, S. Stankovich, I. Jung, D. A. Field, C. A. Ventrice and R. S. Ruoff, *Carbon,* 2009, 47, 145-152.
42. D. Long, W. Li, L. Ling, J. Miyawaki, I. Mochida and S. H. Yoon, *Langmuir,* 2010, 26, 16096-16102.
43. S. Navalon, A. Dhakshinamoorthy, M. Alvaro and H.Garcia, *Chem. Rev.,* 2014, 114, 6179-6212.
44. L. Wang, A. Ambrosi and M. Pumera, *Angew. Chem. Int. Ed.,* 2013, 52, 13818-13821.
45. C. Su, M. Acik, K. Takai, J. Lu, S. J. Hao, Y. Zheng, P. Wu, Q. Bao, T. Enoki, Y. J. Chabal and K. P. Loh, *Nat. Commun.,* 2012, 3, 1298.
46. D. R. Dreyer, H. P. Jia and C. W. Bielawski, *Angew. Chem. Int. Ed.,* 2010, 49, 6813-6816.

Graphical Abstract